RSC Advances

ROYAL SOCIETY OF CHEMISTRY

www.rsc.org/advances

Cite this: DOI: 10.1039/c0xx00000x

www.rsc.org/xxxxxx

PAPER

Influence of amine additives on morphology and phase of antimony(III) oxide nanostructures and study of their optical properties

Fatemeh Behnoudnia[a] and Hossein Dehghani[a]*

Received (in XXX, XXX) Xth XXXXXXXXX 20XX, Accepted Xth XXXXXXXXX 20XX
DOI: 10.1039/b000000x

Antimony trioxide nanostructures were synthesized by a hydrothermal reaction in presence of various amines. The effect of the reaction temperature, the reaction time and kind of amine were investigated on the formation and morphology of antimony trioxide nanostructures. The morphology, structure and properties of synthesized products were characterized using X-ray diffraction, scanning electron microscopy, energy dispersive X-ray spectroscopy and fourier transform infrared spectroscopy. The various morphologies have been observed with changing amines. The broom-like morphology was obtained by adding tetramethylethylenediamine to aqueous solution of antimony trichloride. Depending on the reaction conditions, the nanosheets of antimony trioxide could be produced in the form of pure orthorhombic and also the micro-sized octahedra morphology had cubic phase. The formation of both, the orthorhombic and the cubic polymorphs, were conform by different spectroscopies. We could also obtain both pure cubic phase and orthorhombic phase with changing temperature and using 1,2-diaminocyclohexane and ethylenediamine. Furthermore, the optical properties of synthesized antimony trioxide nanostructures were investigated by photoluminescence and diffuse reflectance spectroscopy.

Introduction

As a result of extensive applications of semiconductors, enormous efforts have been done on synthesis and characterization of these compounds. The properties of materials are related not only to their chemical compositions, but also to their size and morphology. Therefore controlling the shape and size of nanomaterials has been the subject of considerable interest in recent years. Nevertheless, finding a facile and straight away technique to synthesize a desirable morphology is a challengeable task for scientists.

One of the most interesting semiconductors is antimony trioxide (Sb_2O_3) that is used in optoelectronic devices such as LEDs, laser diodes and conductive materials.[1-5] Sb_2O_3 is also applied as flame retardant, a white pigment, adhesives, textile back coating and cumulative drug.[6-9] Therefore these attractive applications of Sb_2O_3 were the main our tendency to do research on synthesis and considering the properties of Sb_2O_3 in nanoscale.

Many methods have been developed to produce nanomaterials, such as sol-gel,[10] gas condensation,[11] hydrothermal,[12-15] vacuum evaporation method,[16] electrochemical method[17] and other things.[18-23] Among these methods, hydrothermal and solvothermal approaches have great advantages in synthesis of Sb_2O_3 crystals through low temperature and simple equipment. Thus these methods are more suitable and economic for large-scale productions.

There are some reports on the preparation of Sb_2O_3 with structural diversity such as fibrils and tubules microstructures,[24] nanoparticles,[25] nanobelts[26] and others morphologies. Wang et al. applied cationic surfactant cetyltrimethylammonium bromide (CTAB) as reagent of self-assembly to provide hollow spindle-like and cobblestone-like microstructure.[27] Recently, Ge et al. have presented a method to assembly of nanowires and produced microspheres of Sb_2O_3 by adding polyvinylpyrrolidone (PVP).[28] Furthermore three dimensional (3D) structures can be considered as nanostructures if they involve the 0D, 1D or 2D nanostructures. The 3D nanostructures have attracted considerable interest in the last few years.[29-34]

Since Sb_2O_3 is a useful optical material, besides the explanation of new types of synthesis procedures, the structural and morphological characterizations samples is necessary, we investigated the optical properties of this material by photoluminescence and DRS methods. Generally, the band gap energy values of Sb_2O_3 reported almost forty years ago are: 3.3 and 4.0 eV for orthorhombic and cubic crystal form, respectively.[35,36] It is noticeable that PL spectra of orthorhombic Sb_2O_3 nanowires and nanobelts, which have an optical band gap of 3.3 eV, show a single band peaked at 375 nm (3.3 eV), corresponding to the band edge, under excitation with 325 nm light.[37,38] Similar PL spectra were found for orthorhombic hierarchical Sb_2O_3 structures.[39]

In this study, Sb_2O_3 nanosheets were synthesized by a simple hydrothermal method which is controllable, facile and the most convenient. Finally the flower-like and the broom-like nanostructures were obtained by self-assembly process. In order to control the morphology of Sb_2O_3 nanostructures, organic additives such as ethylenediamine (EDA), 1,2-diaminocyclohexane (DACH) and tetramethylethylenediamine (TMEDA) were added into reaction solution.

Experimental

Antimony trichloride ($SbCl_3$), ethylenediamine, 1,2-diaminocyclohexane and tetramethylethylenediamine were purchased from Merck. Deionized water was used throughout the experiments. As a general procedure, 0.2 g antimony trichloride was dissolved in 10 ml deionized water under constant stirring. In this time a white precipitation was observed. Then appreciate amount of TMEDA was added dropwise until pH value increased between 8 and 9 to remove formed HCl in solution. After stirring for 15 minutes, the mixture was transferred into an autoclave (25 ml) and maintained at 80-160 °C for 8-48 h. After completing reaction, product was cooled at room temperature and the white solid residue was filtered and washed sufficiently with double distilled water and ethanol. Finally, the precipitate was dried in air at 60 °C for 6 h. For investigation of effect of different bases, this reaction was repeated by using EDA and DACH instead of TMEDA. Furthermore, the reaction temperature and reaction time were studied. Table 1 shows all synthesized samples under different conditions.

Table 1 Experimental parameters for the synthesized samples

Sample	Amine	Temperature/°C	Time/h
S1	TMEDA	120	8
S2	TMEDA	120	16
S3	TMEDA	120	24
S4	TMEDA	120	48
S5	TMEDA	80	16
S6	TMEDA	160	16
S7	DACH	120	16
S8	EDA	120	16

The prepared Sb_2O_3 nanopowders were characterized using an X-ray diffraction (XRD, Phillips X'Pert PRO) equipped with a Cu Kα source having a scanning range of 0–80 Bragg's angle. The morphology of the synthesized products was observed directly by a Philips XL-30ESEM scanning electron microscope (SEM) equipped with energy dispersive X-ray spectroscopy (EDS). Photoluminescence spectra were recorded on PL spectrophotometer Perkin Elmer LS55 using Xe light at 392 nm. Fourier transform infrared (FT-IR) spectra were recorded with a Magna 550 Nicolet instrument (using KBr pellets). Investigation of optical property was carried out by UV-1800 spectrophotometer.

Results and discussion

XRD patterns of the synthesized product had a good agreement with antimony trioxide. Fig. 1 shows the XRD pattern of the prepared Sb_2O_3 samples with TMEDA in 120 °C and different reaction times. Two phases can be observed in the samples, cubic phase Sb_2O_3 (JCPDS # 71-0365) and orthorhombic phase Sb_2O_3 (JCPDS # 71-0383). It is clearly that the cubic phase is almost the major phase but the orthorhombic phase is observed in all samples. There is the orthorhombic phase of Sb_2O_3 in S1, S2 and S3 for the reaction time of 8, 16 and 24 h (Fig. 1a-c). This phase is almost disappeared after 48 h. Therefore increasing the reaction time to 48 h is effective. This figure shows that the obtained Sb_2O_3 in presence of TMEDA has cubic phase.

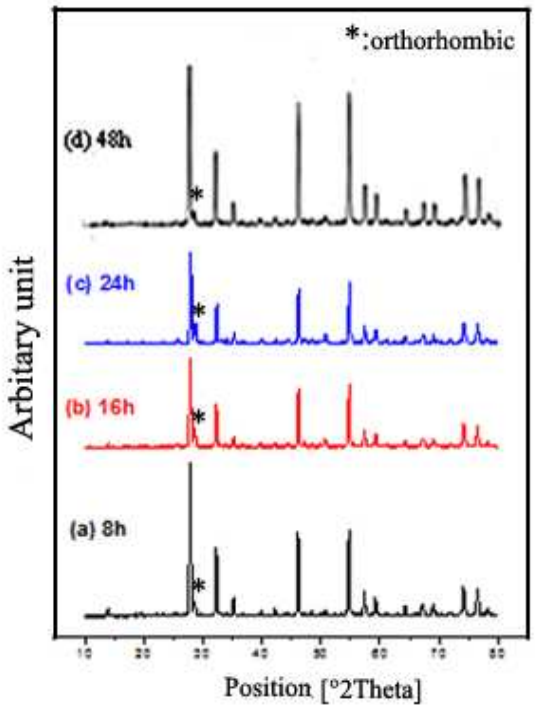

Fig. 1 XRD patterns of Sb_2O_3 samples obtained at presence of TMEDA with different reaction times (a) S1, (b) S2, (c) S3, and (d) S4. *: orthorhombic phase

On the other hand, the reaction temperature was considered. It was observed that increasing temperature causes to increase the orthorhombic phase. However, the XRD pattern (Fig. 2) illustrates that the product is not pure in 160 °C and is included cubic and orthorhombic phases.

So the pure cubic phase can be obtained with increasing the reaction time to 48 h in 120 °C (Fig. 1d). Meanwhile, we found that amines play an important role in the preparation process of Sb_2O_3 and therefore we used various amines in synthesis process. The interesting note is that the pure orthorhombic phase for Sb_2O_3 (JCPDS # 71-0383) was obtained by replacing TMEDA with EDA or DACH. The typical X-ray diffraction (XRD) pattern of the synthesized samples (S7 and S8) was displayed in Fig. 3.

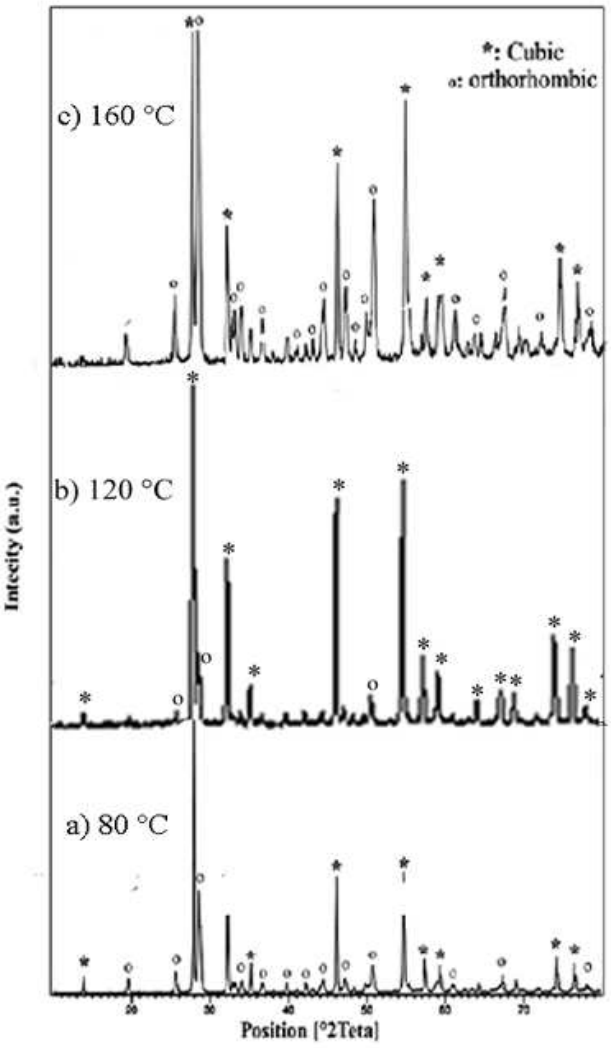

Fig. 2 XRD patterns of Sb_2O_3 samples obtained at presence of TMEDA with different reaction temperatures (a) S5, (b) S2 and (c) S6

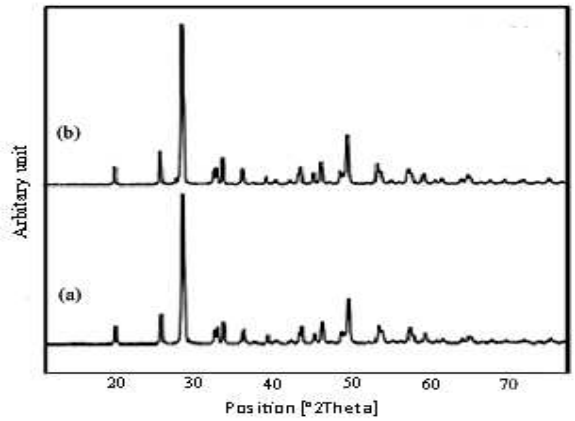

Fig. 3 XRD patterns of Sb_2O_3 samples prepared with different amines (a) DACH (S7) and (b)EDA (S8)

Therefore the pure cubic phase of Sb_2O_3 was obtained by increasing the reaction time and the pure orthorhombic phase of Sb_2O_3 was prepared by changing diamines. The reaction temperature and the type of amine play key roles in the formation process and in result on the morphology of the products.

For further characterization we used SEM to observe the morphology of synthesized Sb_2O_3. Fig. 4 presents the SEM photographs of the prepared Sb_2O_3 with TMEDA in 120 °C at different reaction times. S2 includes nanosheet parts and has the broom-like nanostructure morphology (Fig. 4c, 4d). These structures were seen in the form of broom-like nanostructures. On the other hand, when the reaction time was more than 16 h (S3 and S4) the amount of nanosheets decreased and the prepared products changed to micro-sized Sb_2O_3 octahedra. As shown in Fig. 4e and 4f, the micro-sized Sb_2O_3 octahedra was produced in 120 °C at 24 h completely, while for S1 was observed that the nanosheets were formed incompletely (Fig. 4a and 4b). Also studying the reaction temperature indicated that higher or lower temperature than 120 °C (S5 and S6) were not suitable for the expected morphology. Therefore the optimized condition for preparation of the nanostructures is similar to synthesis condition of S2. Then in similar conditions other amines used for synthesis of the nanostructures. Fig. 5 displays the SEM images of the prepared Sb_2O_3 with DACH (S7) and EDA (S8) in optimized condition. It can be observed that the flower-like nanostructures were obtained in presence of EDA and DACH while the broom-like nanostructure with TMEDA was produced from self-assembly nanosheets (Fig. 5).

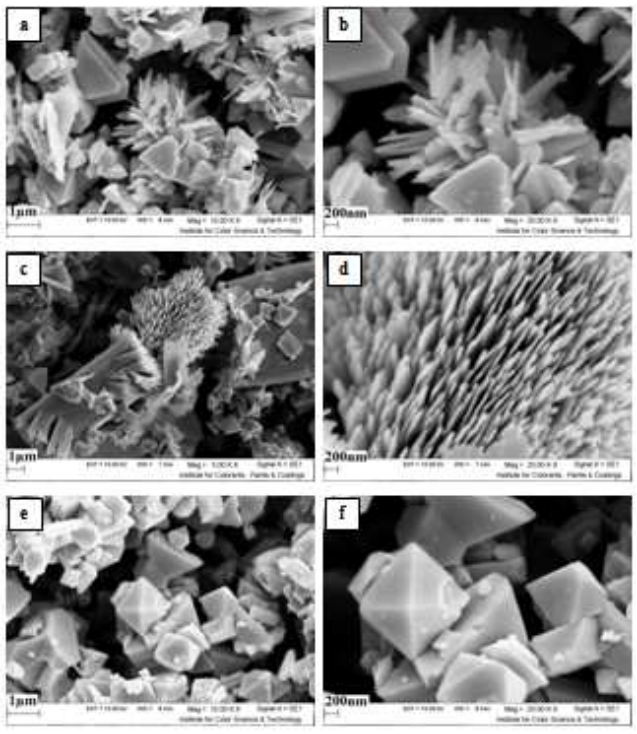

Fig. 4 SEM images of Sb_2O_3 products obtained with TMEDA at the different reaction times (a,b) 8 h (S1), (c,d) 16 h (S2), and (e,f) 24 h (S3)

The orthorhombic phase is consisting of pairs -Sb-O-Sb-O- chains[40]. We suggest that DACH and EDA can attach to Sb

cations because these amines have less steric effect than TMEDA so this attachment makes to form orthorhombic phase that build in chain structure. In fact the cubic phase forms from bicyclic cages[41] that growth in three dimensions. This phase produces in presence of TMEDA which cannot attach to Sb ions, and OH^- can link in 3 dimensions therefore Sb_2O_3 cages produce.

The graphs of EDS analysis for all samples showed only two peaks related to Sb and O (Fig. 6). It was detected no peaks related to other elements or impurities. We obtained energy dispersive X-ray spectrum for all the samples of Sb_2O_3. But all the spectra were similar to Fig. 6.

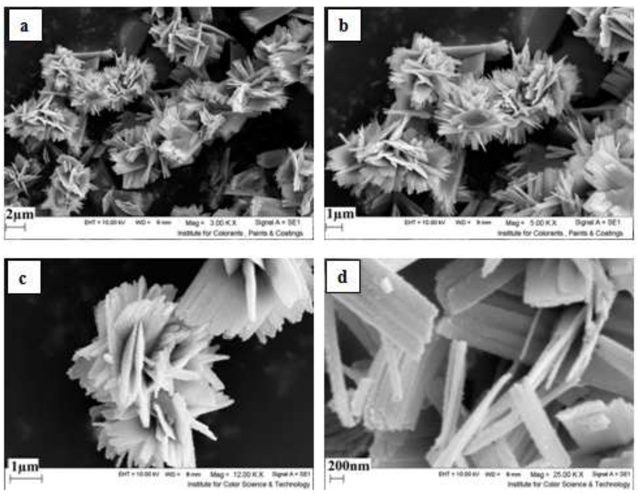

Fig. 5 SEM images of obtained Sb_2O_3 with different amines (a,b) DACH (S7) and (c,d) EDA (S8)

Consequently, antimony trichloride was completely hydrolyzed and was produced Sb_2O_3. Therefore the chemical reactions for the formation of Sb_2O_3 can be expressed as the following:

$$2SbCl_3 + 3H_2O \xrightarrow{\text{Amine}} Sb_2O_3 + 6HCl$$

Fig. 7 shows the PL spectra for Sb_2O_3 excited by 390 nm light beam. Photoluminescence was used for studying the optical properties of the synthesized Sb_2O_3. In particular, there are few reports on luminescence properties, due to its low emission efficiency. The PL spectra of the synthesized Sb_2O_3 were measured at room temperature with an excited wavelength of 390 nm. For comparison, the PL spectra of the as-prepared Sb_2O_3 on flower-like (S7) and also the broom-like (S2) morphologies have been presented in Fig. 7. These samples show an intense peak with the maximum wavelength at 540 nm (S3) and 388 nm (S7). Photoluminescence properties of these samples attribute to oxygen vacancy related to defect emission. From these results, it can be pointed out that the morphology of Sb_2O_3 does not have significant effect for the PL properties and amount of band gap is equal to 3.3 eV for bulk Sb_2O_3 but the band gap of Sb_2O_3 nanostructures was reported in other papers similarly.[37-39] This agrees with our observations of the DRS band in samples.

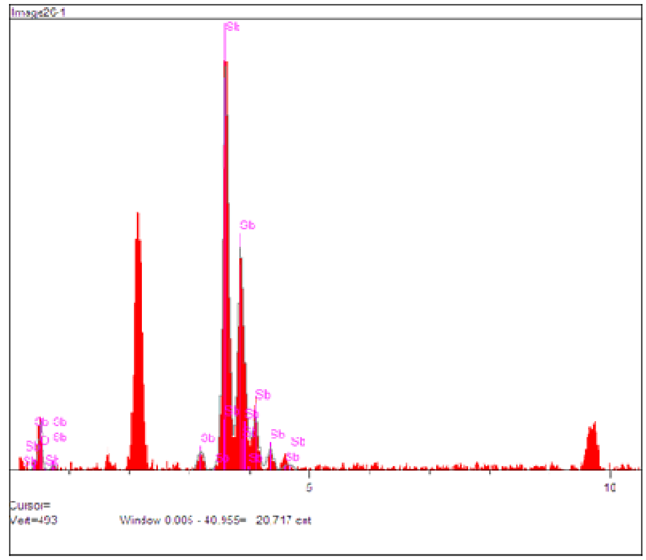

Fig. 6 EDX spectrum of Sb_2O_3 obtained with EDA (S8)

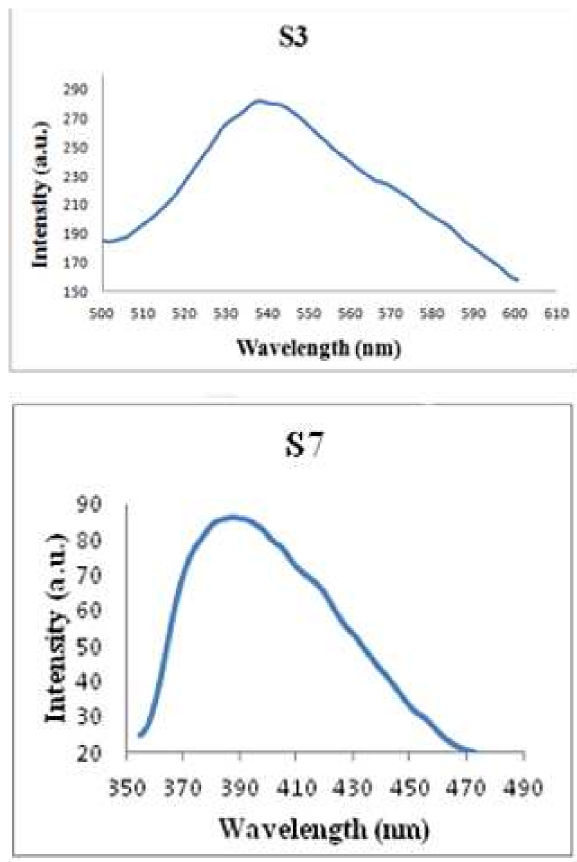

Fig. 7 Photoluminescence spectra of the synthesized Sb_2O_3 at λ_{ex} = 390 nm S3 and S7

For investigation of optical properties, diffuse reflectance spectroscopy (DRS) was used for S3, S7 and S8. The energy band gap was estimated by assuming a direct transition between valence and conduction band of Sb_2O_3 nanostructures. In order to determine the direct optical band gap was used the plotting the dependence of $(\alpha h\nu)^2$ versus $h\nu$, as shows in Fig. 8.The value of optical band gap can be determined by extrapolating the linear

portion of this plot to $(\alpha h\nu)^2 = 0$. It was found that the optical band gap for orthorhombic phase samples S7 and S8 is 3.3 eV but for S3 with cubic phase, band gap was calculated 3.92 eV, the obtained values of optical band gap are in good agreement with those values reported previously for Sb_2O_3. In comparison with PL, the calculated band gap from PL spectrum is rather less than DRS.

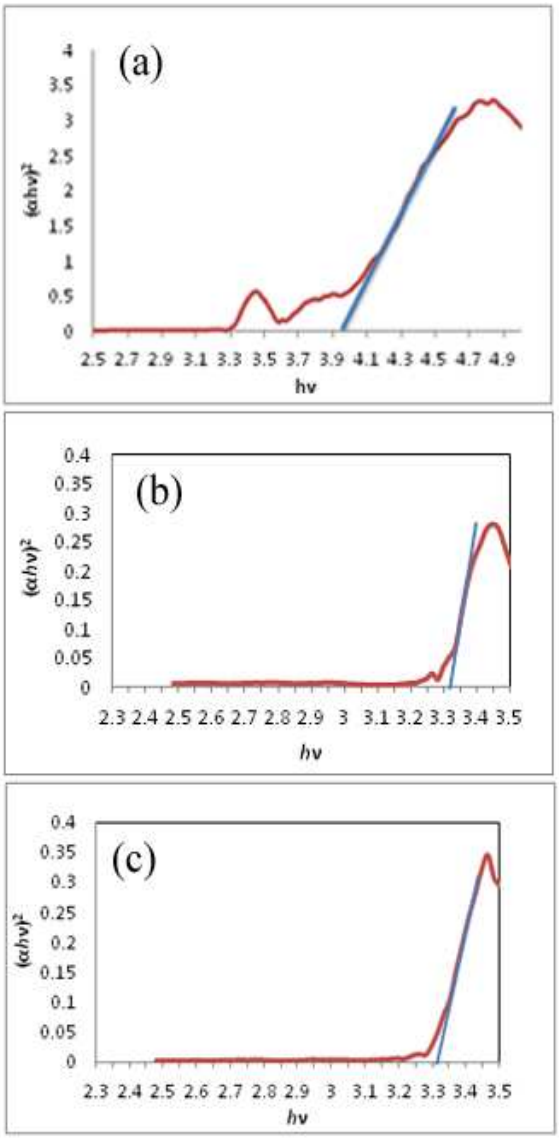

Fig. 8 Plots (α h ν)^2 vs. h ν for Sb_2O_3 nanostructures by DRS: (a) S3, (b) S7 and (c) S8

Comparison of the FT-IR spectra for both pure phases of Sb_2O_3 (S3 and S7) were shown in the Fig. 9. In this figure, it observes an absorption band at 3400 cm^{-1} related to the stretching vibration of (O–H) for the adsorbed water on the surface of Sb_2O_3. The observed peak at 1630 cm^{-1} is due to bending vibration of H_2O. According to literatures, the region of 750 cm^{-1} to 300 cm^{-1} can be related to the stretching vibrations of Sb–O. The intense band at 735 cm^{-1} assigned to symmetric combinations of stretching vibrations (Sb–O) in the cubic phase which reveals at 690 cm^{-1} in the orthorhombic. A doublet contain both of frequencies is observed in the mixed sample. In the IR spectrum of the orthorhombic antimony trioxide, a doublet band is already seen at 550-400 cm^{-1}. This doublet is assigned to symmetric and asymmetric combinations of stretching vibration of Sb–O–Sb and oxide bridge functional group (O–Sb–O) in Sb_2O_3. Intensities of these peaks decrease remarkably in the cubic phase which they are related to asymmetric combinations of stretching in the Sb–O–Sb. Another peak at 457 cm^{-1} is also related to symmetric and asymmetric combinations of stretching of Sb–O–Sb bonds that occurring in the chain plane of orthorhombic phase. This peak disappears in the cubic sample (S3). The bands under 460-360 cm^{-1} correspond to vibrations caused by the deformation of Sb–O–Sb bonds.[42]

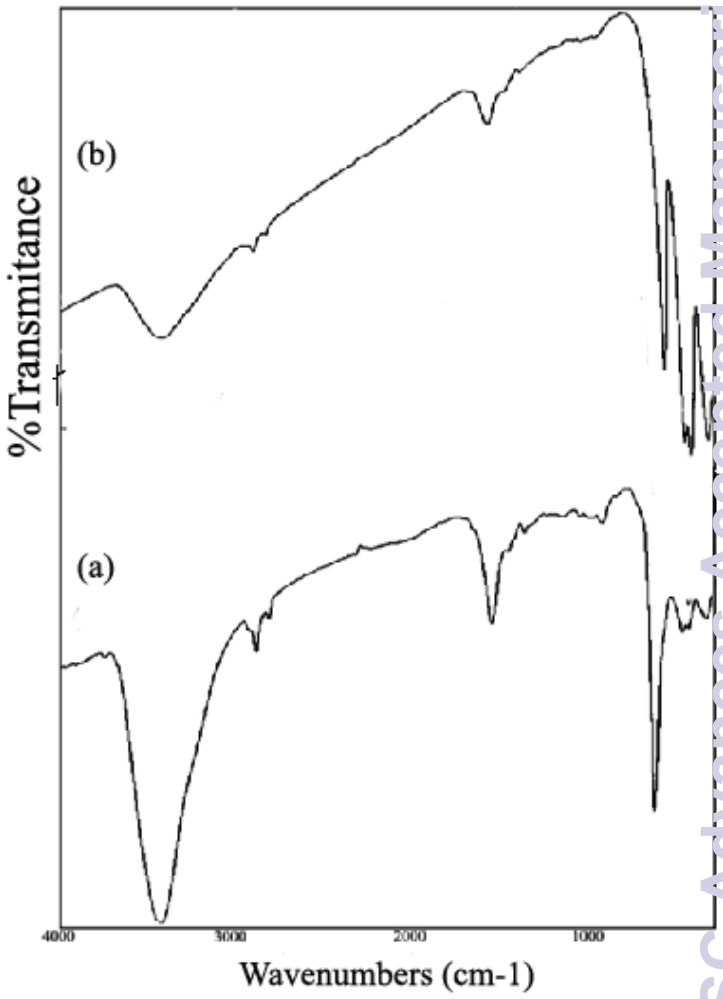

Fig. 9 FT-IR spectra of Sb_2O_3 in (a) the cubic phase (S3) and (b) the orthorhombic phase (S7)

Conclusions

In summary, a simple, inexpensive and single-step method has been developed for the synthesis of antimony trioxide (Sb_2O_3). In this work, the crystallinity and morphology of Sb_2O_3 have been controlled. The reaction temperature has a strong effect on the structure and morphology of the obtained Sb_2O_3 nanostructures. On the other hand, type of amine influences the purity and the phase of the prepared Sb_2O_3. Depending on the reaction

conditions, Sb_2O_3 nanosheets could be produced in the form of pure orthorhombic and micro-sized octahedra in cubic polymorphs. The formation of both, the orthorhombic and the cubic polymorphs, were conform by SEM, XRD, FT-IR, PL and DRS spectroscopies.

Acknowledgments

The authors are grateful to University of Kashan for supporting this work by Grant No. (159183/12).

[a] *Department of Inorganic Chemistry, Faculty of Chemistry, University of Kashan, Kashan, I.R. Iran. Fax: +98 315 591 2397; Tel: +98 315 591 2386; E-mail: dehghani@kashanu.ac.ir*

References

1. T. Som, B. Karmakar, *J. Lumin*., 2008, 128, 1989.
2. H. Jiang, J. Q. Hu, F. Gu, C. Z. Li, *J. Phys. Chem. C,* 2008, 112, 12138.
3. H. X. Li, M. X. Xia, G. Z. Dai, H. C. Yu, Q. L. Z.hang, A. L. Pan, T. H. Wang, Y. G. Wang, B. S. Zou, *J. Phys. Chem. C*, 2008, 112, 17546.
4. H. Bryngelsson, J. Eskhult, L. Nyholm, M. Herranen, O. Alm, K. Edström, *Chem. Mater.*, 2007, 19, 1170.
5. B. Duh, *Polymer*, 2002, 43, 3147.
6. M. Z. Xue, Z. W. Fu*, Electrochem. Commun.,* 2006, 8, 1253.
7. K. Ozawa, Y. Sakka, A. Amamo, *J. Mater. Res.,* 1998, 13, 830.
8. J. H. Youk, R. P. Kambour, W. J. MacKnight, *Macromolecules,* 2000, 33, 3594.
9. Y. X. Zhang, G. H. Li, L. D. Zhang, *Chem. Lett.,* 2004, 33, 334.
10. J. F. Brazdil, M. A. Toft, J. P. Bartek, R. G. Teller, R. M. Cyngier, *Chem. Mater.,* 1998, 10, 4101.
11. D. W. Zeng, C. S. Xie, B. L. Zhu, W. L. Song, *Mater. Lett.,* 2004, 58, 312.
12. H. Jiang, J. Q. Hu, F. Gu, W. Shao, C. Z. Li, *Chem. Commun.*, 2009, 3618.
13. Z. T. Deng, F. Q. Tang, D. Chen, X. W. Meng, L. Cao, B. S. Zou, *J. Phys. Chem. B,* 2006, 110, 18227.
14. H. Jiang, J. Q. Hu, F. Gu, C. Z. Li, *J. Phys. Chem. C,* 2008, 112, 12139.
15. L. Liu, Z. L. Hu, Y. M. Cui, B. Li, X. F. Zhou, *Solid State Sci.*, 2010, 12, 882.
16. K. Q. Qiu, R. L. Zhang, *Vacuum,* 2006, 80, 1017.
17. S. Mohan, S. Pushpavanam, S. Vasudevan, *Ind. Eng. Chem. Res.,* 2007, 46, 7871.
18. A. H. Abdullaha, N. H. M. Noora, I. Ramli, M. Hashim, *Mater. Chem. Phys.*, 2008, 111, 202.
19. Y. W. Jun, M. F. Casula, J. H. Sim, S. Y. Kim, J. Cheon, A. P. Aliyisatos*, J. Am. Chem. Soc.,* 2003, 125, 15981.
20. Y. Zhao, Z. Zhang, W. Liu, H. Dang, Q. Xue, *J. Am. Chem. Soc.,* 2004, 126, 6854.
21. Z.L. Zhang, L. Guo, W.D. Wang, *J. Mater. Res.,* 2001, 16, 803.
22. L. Guo, Z. H. Wu, T. Liu, W. D. Wang, H. S. Zhu, *Chem. Phys. Lett.,* 2000, 318, 49.
23. S. Friedrichs, R. R. Meyer, J. Sloan, A. I. Kirkland, J. L. Hutchison, M. L. H. Green, *Chem. Commun.,* 2001, 929.
24. C. Ye, G. Meng, L. Zhang, G. Wang, Y. Wang, *Chem. Phys. Lett.*, 2002, 363, 34.
25. B. Pillep, P. Behrens, *J. Phys. Chem. B,* 1999, 103, 9595.
26. B.S. Naidu, M. Pandey, V. Sudarsan, R.K. Vatsa, R. Tewari, *Chem. Phys. Lett.,* 2009, 474, 180.
27. S. Ge, Q. Wang, Q. Shao, Y. Zhao, X. Yang, X. Wang, *Appl. Surf. Sci.,* 2011, 257, 3657.
28. Q. Wang, S. Ge, Q. Shao, Y. Zhao, *Physica B*, 2011, 406, 731.
29. Z. Sun, J.H. Kim, Y. Zhao, F. Bijarbooneh, V. Malgras, Y. Lee, Y.M. Kang, S.X. Dou, *J. Am. Chem. Soc.,* 2011, 133, 19314.
30. S. Xiong, B. Xi, C. Wang, G. Zou, L. Fei, W. Wang, Y. Qian, *Chem. A Eur. J.,* 2007, 13, 3076.
31. W. Zhang, L. Xu, Kaibin Tang, F. Li. Y. Qian, Eur. *J. Inorg. Chem.,* 2005, 2005, 653.
32. C. Wu, Y. Xie, D. Wang, J. Yang, T. Li, *J. Phys. Chem. B,* 2003, 107, 13583.
33. P. Yu, X. Zhang, D. Wang, L. Wang, Y. Ma, *Cryst. Growth Des.,* 2009, 9, 528
34. Z. Zhao, F. Geng, J. Bai, H.M. Cheng, *J. Phys. Chem. C,* 2007, 111, 3848.
35. B. Wolffing, Z. Hurych, *Phys Status Solidi (a),* 1973, 16, K161.
36. C. Wood, B. Van Pelt, A. Dwight, *Phys Status Solidi(b),* 1972, 54, 701.
37. Z. Deng, F. Tang, D. Chen, X. Meng, L. Cao, B. Zou, *J. Phys. Chem. B,* 2006, 110, 18225.
38. Y. Zhang, G. Li, J. Zhang, L. Zhang, *Nanotechnology,* 2004, 15, 762.
39. G. Fan, Z. Huang, C. Chai, D. Liao, *Mater. Lett.,* 2011, 65, 1141.
40. C. Svensson, *Acta Cryst.,* 1974, B30, 458.
41. C. Svensson, *Acta Cryst.,* 1975, B31, 2016.
42. E. I. Voit, A. E. Panasenko, L. A. Zemnukhova, *J. Struct. Chem.,* 2009, 50, 60.